CLUSTER ANALYSIS OF VOLCANOES ON IO: IMPLICATIONS FOR TIDAL HEATING AND MAGMA ASCENT. C. W. Hamilton[1], C. D. Beggan[2], S. Still[3], M. Beuthe[4], R. M. C. Lopes[5], D. A. Williams[6], J. Radebaugh[7], and W. Wright[3], [1]NASA Goddard Space Flight Center, Greenbelt, MD, USA (christopher.hamilton@nasa.gov), [2]British Geological Survey, Edinburgh, UK, [3]Univ. of Hawai'i at Mānoa, Honolulu, HI, USA, [4]Royal Observatory of Belgium, Brussels, Belgium, [5]Jet Propulsion Laboratory, California Institute of Technology, Pasadena, CA, USA, [6]Arizona State Univ., Tempe, AZ, USA, [7]Brigham Young Univ., Provo, UT, USA.

Introduction: Extreme volcanism on Io results from tidal heating, but its tidal dissipation mechanisms and magma ascent processes are poorly constrained. The relative strength of tidal heating in the asthenosphere and deep-mantle greatly affect expected patterns of surface heat flux. Assuming volcanoes are correlated with surface heat flux, their distribution may be used to distinguish between tidal heating models. Here we analyze the distribution of volcanoes identified within the first 1:15,000,000-scale global geologic map of Io [1] to test tidal heating models.

Background: Io, the innermost of Jupiter's Galilean satellites, is the most volcanically active body in the Solar System. Io's global mean heat flow of ~2 W m^{-2} [2] is ~20 times larger than the Earth's. However, unlike the Earth, Io's internal heat comes primarily from the dissipation of tidal energy [3]. In end-member tidal dissipation models (Fig. 1), the bulk of Io's heating occurs either within the deep-mantle or within the asthenosphere [4–7], while in mixed models heating is partitioned between these end-members [7, 8].

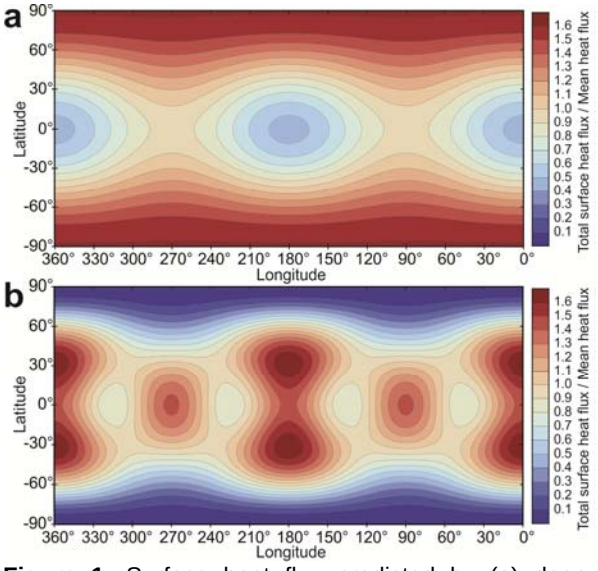

Figure 1. Surface heat flux predicted by (**a**) deep-mantle and (**b**) asthenospheric-heating end-members.

In deep-mantle heating models, surface flux is maximum near the poles and minimum at the equator, with absolute minima occurring at the subjovian and antijovian points (Fig. 1a). In asthenospheric models, heat flux is minimum at the poles and maximum at low latitudes, with primary maxima occurring near the subjovian and antijovian points (at approximately ±30° latitude), and near the leading and trailing points (Fig. 1b). Spatial variations in surface heat flux are lower in mixed models, with maxima migrating towards the poles as deep-mantle heating is added to asthenospheric heating. Moderate convection does not fundamentally change these patterns, but more vigorous convection induces horizontal flows that smooth lateral variations.

Methodology: *Interior models.* Surface heat flux patterns in Figure 1 are computed based on [6, 9]. In these models, we treat Io as a spherically symmetric incompressible body with Maxwell rheology and solve the deformation equations with the propagator matrix technique. The heat flows radially to the surface. We adopt the parameters of [6], except for the shear modulus μ and viscosity η, which are adjusted to generate the correct total power [10]. In the deep-mantle end-member heating model (Fig. 1a), $\mu = 3.5 \times 10^9$ Pa and $\eta = 10^{15}$ Pa · s. In the asthenospheric end-member model (Fig. 1b), $\mu = 4 \times 10^4$ Pa and $\eta = 10^{10}$ Pa · s, assuming a 50 km-thick asthenosphere.

Distance-based clustering. We analyzed 173 hotspots and 529 patera floor units identified by spacecraft and Earth-based telescopes [1]. Hotspots are thermal anomalies associated with active volcanoes, whereas paterae are volcanic-tectonic depressions that are interpreted to be analogous to terrestrial calderas [11]. We partition hotspots and paterae into k clusters by iteratively assigning them to cluster centers and relocating the cluster centers to minimize the total great circle distance between all points and their nearest cluster center. Distance minimization algorithms are prone to identifying local minima (i.e., suboptimal solutions), and so we use an optimization technique known as deterministic annealing [12] to search for the global optimum. In two cluster solutions (k = 2), polar clusters would imply deep-mantle heating (Fig. 1a), whereas clusters at low latitudes would imply asthenospheric-dominated tidal heating (Fig. 1b). Solutions with six clusters (k = 6) are important because asthenospheric-dominated tidal heating models predict six surface heat flux maxima (Fig. 1b).

Results: Distance-based clustering using k = 2 identifies hotspot concentrations at 17.8ºS, 317.6ºW and 12.7ºN, 136.6ºW (Fig. 2a), whereas patera cluster centers are located at 15.6ºS, 320.5ºW and 1.1ºN, 149.5ºW (Fig. 2b). Coordinates for the k = 6 hotspot cluster centers are: 41.6ºN, 302.0ºW; 45.6ºS, 294.5ºW;

9.5ºN, 214.5ºW; 37.0ºS, 146.5ºW; 28.0ºN, 114.6ºW; and 2.3ºS, 22.0ºW (Fig. 2c). Cluster centers for the k = 6 paterae solution are located at: 3.0ºN, 333.4ºW; 65.2ºS, 300.9ºW; 22.8ºN, 249.2ºW; 22.2ºS, 176.9ºW; 33.5ºN, 135.2ºW; and -20.0ºS, 77.1ºW (Fig. 2d). Uncertainties in cluster center locations are approximately 121 km for hotspots k = 2, <1 km for paterae k = 2, 262 km for hotspots k = 6, and 92 km for paterae k = 6.

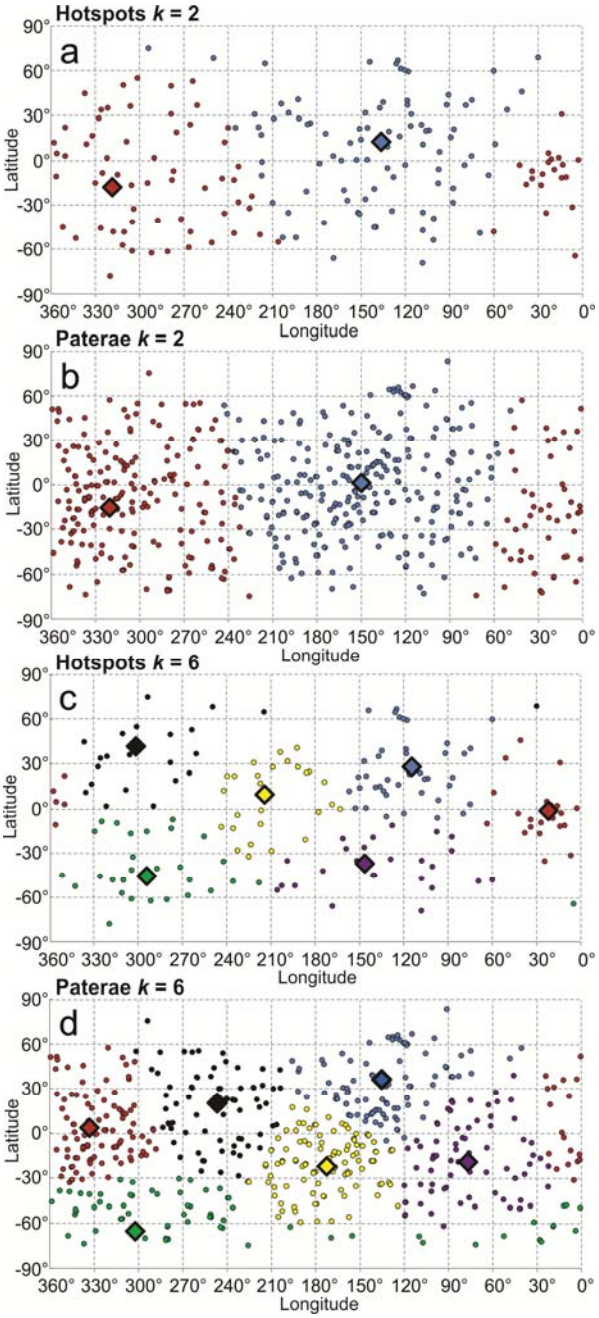

Figure 2. Clustering results using two clusters (k = 2) for (**a**) hotpots and (**b**) paterae. Results with six clusters (k = 6) for (**c**) hotpots and (**d**) paterae. Diamonds represent cluster centers and circles represent volcanic centers. Shared colors indicate cluster membership.

Discussion: Concentration of volcanoes at low latitudes supports a dominant role for asthenospheric heating. However, there is a significant ~30–60° eastward offset in the k = 2 and 6 hotspot clustering solutions (Figs. 2a and 2c), relative to surface heat flux maxima predicted by asthenospheric-dominated tidal heating models (Fig. 1b). Nonsynchronous rotation has been invoked as a possible explanation for the eastward offset of paterae from predicted surface heat flux maxima [11, 13]. Alternatively, surface expressions of volcanism may be related to regions favoring magma ascent from an extensive reservoir, such as a global magma ocean [14]. Regions of enhanced volcanism may therefore coincide with zones of weakness related to a combination of crustal heterogeneities and the global state of stress generated by structural, thermal, and orbital processes. If so, the offset between the current tidal axis (i.e., the predicted zone of dominant tidal heating) and the maximum concentrations of active volcanoes may result from significant lateral advection of magma at depth prior to being erupted to the surface. Anisotropies controlling the locations of magma upwelling and enhanced volcanism may include existing fault distributions in the lithosphere and a combination of stresses associated with mantle convection, diapirism, magma chambers, shallow intrusions, volcanic conduits, and tidal flexing.

Conclusions: The overall concentration of volcanoes at mid- to low-latitudes generally supports asthenospheric-dominated tidal heating, but the eastward offset of volcano clusters from the current tidal axis is not predicted by existing tidal heating models. The discrepancy may be explained by faster than synchronous rotation and/or subsurface transport within a global magma ocean from sites of maximum asthenospheric heat production to sites that are more favorable for generating magma ascent.

References: [1] Williams D. A. et al. (2011) *Icarus*, 214, 91–112. [2] Spencer J. R. et al. (2000) *Science*, 288, 1198–1201. [3] Peale et al. (1979) *Science*, 203(4383) 892–894. [4] Ross M. N. and Schubert G. (1985) *Icarus*, 64, 391–400. [5] Schubert G. et al. (1986) In: *Satellites*, Univ. of Arizona Press, 224–292. [6] Segatz M. et al. (1988) *Icarus*, 75, 187–206. [7] Tackley P. J. et al. (2001) *Icarus*, 149, 79–93. [8] Ross M. N. et al. (1990) *Icarus*, 85, 309–325. [9] Tobie G. et al. (2005) *Icarus*, 177, 534–549. [10] Spohn T. (1997) In: *Tidal Phenomena*, Springer Verlag, 66, 345–377. [11] Radebaugh J. et al. (2001) *J. Geophys. Res.*, 106, 33005–33020. [12] Rose K. (1990) *Proceedings of the IEEE*, 86, 11, 2210–2239. [13] Schenk P. M. et al. (2001) *J. Geophys. Res.*, 106, 33201–33222. [14] Khurana, K. K. et al. (2011) *Science*, 332, 1186–1189.